29 frequencies for the delta Scuti variable BI CMi: the 1997-2000 multisite campaigns

M. Breger, Rafael Garrido, Gerald Handler, M. A. Wood, R. R. Shobbrook, K. M. Bischof, F. Rodler, Richard O. Gray, Anamarija Stankov, Patrice Martinez, et al.

Mon. Not. R. Astron. Soc. **329,** 531–542 (2002)

29 frequencies for the δ Scuti variable BI CMi: the 1997–2000 multisite campaigns

M. Breger,[1★] R. Garrido,[2] G. Handler,[1,3] M. A. Wood,[4] R. R. Shobbrook,[5] K. M. Bischof,[1] F. Rodler,[1] R. O. Gray,[6] A. Stankov,[1] P. Martinez,[3] D. O'Donoghue,[3] R. Szabó,[7] W. Zima,[1] A. B. Kaye,[8] C. Barban[9,10] and U. Heiter[1]

[1]*Astronomisches Institut der Universität Wien, Türkenschanzstr. 17, A–1180 Wien, Austria*
[2]*Instituto de Astrofisica de Andalucia, CSIC, Apdo. 3004, E-18080 Granada, Spain*
[3]*SAAO, PO Box 9, Observatory 7935, Cape Town, South Africa*
[4]*Department of Physics and Space Sciences & SARA Observatory, Florida Institute of Technology, Melbourne, FL 32901, USA*
[5]*Department of Physics, University of Sydney, Australia*
[6]*Department of Physics and Astronomy, Appalachian State University, Boone, NC 28608, USA*
[7]*Konkoly Observatory, PO Box 67, H-1525 Budapest XII, Hungary*
[8]*Applied Physics Division, X-5, Los Alamos National Laboratory, Mail Stop F-663, Los Alamos, NM 87545, USA*
[9]*Observatoire de Paris, DASGAL, UMR 8633, 92105 Meudon, France*
[10]*National Solar Observatory, 950 N. Cherry, Tucson, AZ 85719, USA*

Accepted 2001 September 6. Received 2001 July 24

ABSTRACT

A multisite campaign of BI CMi was carried out with excellent frequency resolution and high photometric accuracy from 1997 to 2000, including two long observing seasons. 29 pulsation frequencies could be extracted from the 1024 h (177 nights) of photometry used. The detected frequencies include 20 pulsation modes in the main pulsation frequency range from 4.8 to 13.0 cycle d^{-1} (55 to 150 μHz), eight linear combinations of these frequencies, and a very low frequency at 1.66 cycle d^{-1}. Since the value of the low frequency at 1.66 cycle d^{-1} cannot be identified with a linear combination of other frequencies, g-mode pulsation is suspected, but rotational modulation of abundance spots cannot be ruled out. BI CMi, which is situated near the cool edge of the classical instability strip, may be both a δ Scuti and a γ Doradus star. Another outstanding property of BI CMi is the presence of a number of close frequency pairs in the power spectrum with separations as small as 0.01 cycle d^{-1}.

A rotational velocity of $v \sin i = 76 \pm 1\,\mathrm{km\,s^{-1}}$ was determined from a high-dispersion spectrum. From phase differences, the dominant modes can be identified with ℓ values from 0 to 2. The spectral type and evolutionary status of BI CMi are examined.

Key words: techniques: photometric – stars: individual: BI CMi – stars: oscillations – stars: rotation – δ Scuti.

1 INTRODUCTION

The Delta Scuti Network is engaged in ground-based asteroseismology of non-radially pulsating stars. The adopted method recognizes the fact that the successes of helioseismology are a consequence of the large amount of data available. Consequently, for carefully chosen single stars, a maximum of information is obtained with different techniques optimized for specific deductions. At the present time, high-precision photometry between 500 and 1000+ hours is used to derive 30 or more frequencies of pulsation per star. Because of cancellation effects across the stellar surface, the modes detected by photometry have low values of the spherical degree, ℓ. We obtain photometry in at least two wavelength regions, so that the phase differences can be used to identify the ℓ values. Since millimagnitude-accuracy photometry for most δ Scuti stars can be obtained on a telescope of 1 m or smaller, a multisite campaign covering many months of observation can be organized.

BI CMi (HD 66853, F2) is situated near the cool border of the classical instability strip in the Hertzsprung–Russell diagram. The star was chosen for an extensive multisite campaign by the Delta Scuti Network because there exists the possibility that this star might be both a δ Scuti (p modes) and a γ Doradus (g modes) star. The latter group represents a type of pulsation with low frequencies

★E-mail: breger@astro.univie.ac.at

found (mainly) outside the cool border of the classical instability strip. The light variability of BI CMi was discovered by Kurpinska-Winiarska, Winiarska & Zola (1988), when it was used as a comparison star for the eclipsing binary YY CMi.

Mantegazza & Poretti (1994) deduced from the analysis of 16 nights of observation that in addition to the δ Scuti-type frequencies, BI CMi showed two frequencies with very low values, namely, 0.149 and 0.659 cycle d^{-1}. The star might, therefore, present a transition between both types of pulsators (Breger & Beichbuchner 1996). More extensive measurements and analyses are needed to confirm the frequencies, examine possible 1 cycle d^{-1} aliasing and exclude the possibility of other explanations such as the peaks in the power spectrum being caused by combination frequencies, f_i–f_j.

2 NEW PHOTOMETRY

During the time periods 1997 January, 1998 November to 1999 March, as well as 1999 December to 2000 March, the star BI CMi was observed photometrically at six observatories. Both photomutiplier (PMT) and charge-coupled device (CCD) detectors were used. It is customary for DSN campaigns to disregard all data from sites with poor instrumentation, poor weather or other sources of *systematic* errors in excess of 10 mmag. In the present campaign a total of 1024 hours of observations on 177 nights were found to be of high quality, as judged by the constancy of the chosen comparison stars. These observations were retained.

The majority of observations were obtained with standard photoelectric photometers, using photomultiplier tubes as detectors. All

Table 1. Journal of photoelectric measurements of BI CMi.

Start HJD	Length (h)	Obs.	Start HJD	Length (h)	Obs.	Start HJD	Length (h)	Obs.	Start HJD	Length (h)	Obs.
245 0000+			245 0000+			245 0000+			245 0000+		
465.70	6.83	APT	1185.68	8.38	APT	1231.34	6.05	SNO	1553.68	8.19	APT
466.70	4.33	APT	1186.68	8.38	APT	1232.83	1.61	APT	1554.68	8.18	APT
468.69	5.13	APT	1187.67	8.30	APT	1235.61	6.81	APT	1555.67	8.25	APT
476.66	2.71	APT	1188.67	5.32	APT	1236.60	7.03	APT	1556.67	8.18	APT
478.66	2.84	APT	1189.85	3.97	APT	1237.60	6.81	APT	1558.67	3.28	APT
479.63	7.65	APT	1191.39	4.21	SAAO	1238.62	5.11	APT	1559.75	6.13	APT
480.61	8.14	APT	1191.67	8.13	APT	1239.67	4.26	APT	1560.66	3.71	APT
1138.81	5.72	APT	1192.35	5.79	SAAO	1240.61	6.27	APT	1569.63	5.78	APT
1139.80	5.79	APT	1192.76	2.53	APT	1241.60	3.32	APT	1570.66	7.33	APT
1140.80	5.88	APT	1193.75	6.02	APT	1246.62	1.24	APT	1571.63	8.27	APT
1141.84	4.86	APT	1193.99	6.23	SSO	1248.61	5.53	APT	1573.93	0.78	APT
1142.81	5.64	APT	1194.30	4.31	SAAO	1250.61	5.24	APT	1574.62	0.96	APT
1143.80	3.10	APT	1194.85	3.68	APT	1251.62	5.43	APT	1576.62	3.05	APT
1147.93	2.79	APT	1195.68	7.31	SARA	1252.67	2.64	APT	1577.62	7.86	APT
1148.89	3.63	APT	1196.47	1.90	SAAO	1253.62	5.07	APT	1578.75	4.79	APT
1151.77	4.97	APT	1196.65	8.37	APT	1256.62	5.07	APT	1579.60	8.18	APT
1152.77	6.92	APT	1196.70	8.21	SARA	1263.91	3.67	SSO	1580.82	2.97	APT
1153.94	2.67	APT	1196.97	6.65	SSO	1514.79	6.28	APT	1581.61	6.70	APT
1155.76	7.07	APT	1197.65	8.38	APT	1515.78	6.36	APT	1582.60	4.17	APT
1156.76	7.06	APT	1197.64	9.61	SARA	1516.78	6.53	APT	1584.72	5.05	APT
1157.76	0.42	APT	1197.15	0.99	SSO	1517.78	6.54	APT	1585.77	3.91	APT
1159.75	7.30	APT	1198.62	9.79	SARA	1519.77	6.88	APT	1586.61	7.53	APT
1160.75	7.33	APT	1198.65	8.07	APT	1520.81	3.52	APT	1588.60	7.64	APT
1161.74	7.57	APT	1199.69	5.66	SARA	1521.80	1.34	APT	1590.60	7.42	APT
1163.80	5.56	APT	1200.31	6.01	SAAO	1523.76	1.01	APT	1595.60	7.34	APT
1166.17	1.55	SSO	1201.63	9.48	SARA	1524.79	3.34	APT	1601.24	5.12	PIZ
1166.73	1.60	APT	1201.64	8.38	APT	1525.77	6.43	APT	1601.61	6.61	APT
1167.73	5.71	APT	1202.33	5.67	SAAO	1526.75	2.10	APT	1602.23	6.06	PIZ
1169.08	3.57	SSO	1203.36	4.94	SAAO	1529.74	7.10	APT	1602.61	4.69	APT
1169.72	8.08	APT	1204.32	5.12	SAAO	1530.74	7.16	APT	1603.23	6.35	PIZ
1170.03	4.55	SSO	1213.63	2.12	APT	1531.74	3.25	APT	1605.61	6.19	APT
1170.75	5.46	APT	1218.30	8.22	SNO	1532.73	7.41	APT	1606.61	6.18	APT
1171.05	4.11	SSO	1220.30	8.03	SNO	1533.73	7.61	APT	1607.62	6.19	APT
1171.86	4.79	APT	1221.30	7.86	SNO	1535.72	7.72	APT	1612.62	5.73	APT
1172.72	8.25	APT	1222.45	2.27	SNO	1537.72	8.13	APT	1613.65	5.04	APT
1173.71	3.94	APT	1223.56	1.23	SNO	1538.72	4.43	APT	1614.62	5.66	APT
1175.71	8.26	APT	1224.31	7.00	SNO	1539.72	1.85	APT	1615.62	4.12	APT
1176.71	8.24	APT	1225.36	6.23	SNO	1545.70	8.19	APT	1617.72	2.88	APT
1177.70	8.28	APT	1225.59	2.99	APT	1546.70	8.22	APT	1618.64	4.84	APT
1179.70	8.40	APT	1226.30	7.26	SNO	1547.69	8.22	APT	1619.74	2.26	APT
1180.69	8.40	APT	1228.47	3.45	SNO	1548.69	8.19	APT	1620.61	5.36	APT
1181.69	8.38	APT	1229.36	5.43	SNO	1549.69	8.19	APT	1621.61	5.16	APT
1182.69	8.51	APT	1230.31	7.23	SNO	1550.69	7.95	APT	1622.67	3.83	APT
1183.69	8.50	APT	1230.73	4.19	APT	1551.68	8.19	APT	1623.62	4.93	APT
1184.97	1.58	APT									

APT: Arizona; SSO: Siding Spring Observatory, Australia, Shobbrook; SNO: Sierra Nevada, Garrido; SARA: at KPNO, Wood; SAAO: South African Astronomical Observatory; PIZ: Piszkéstető, Szabo, Bischof.

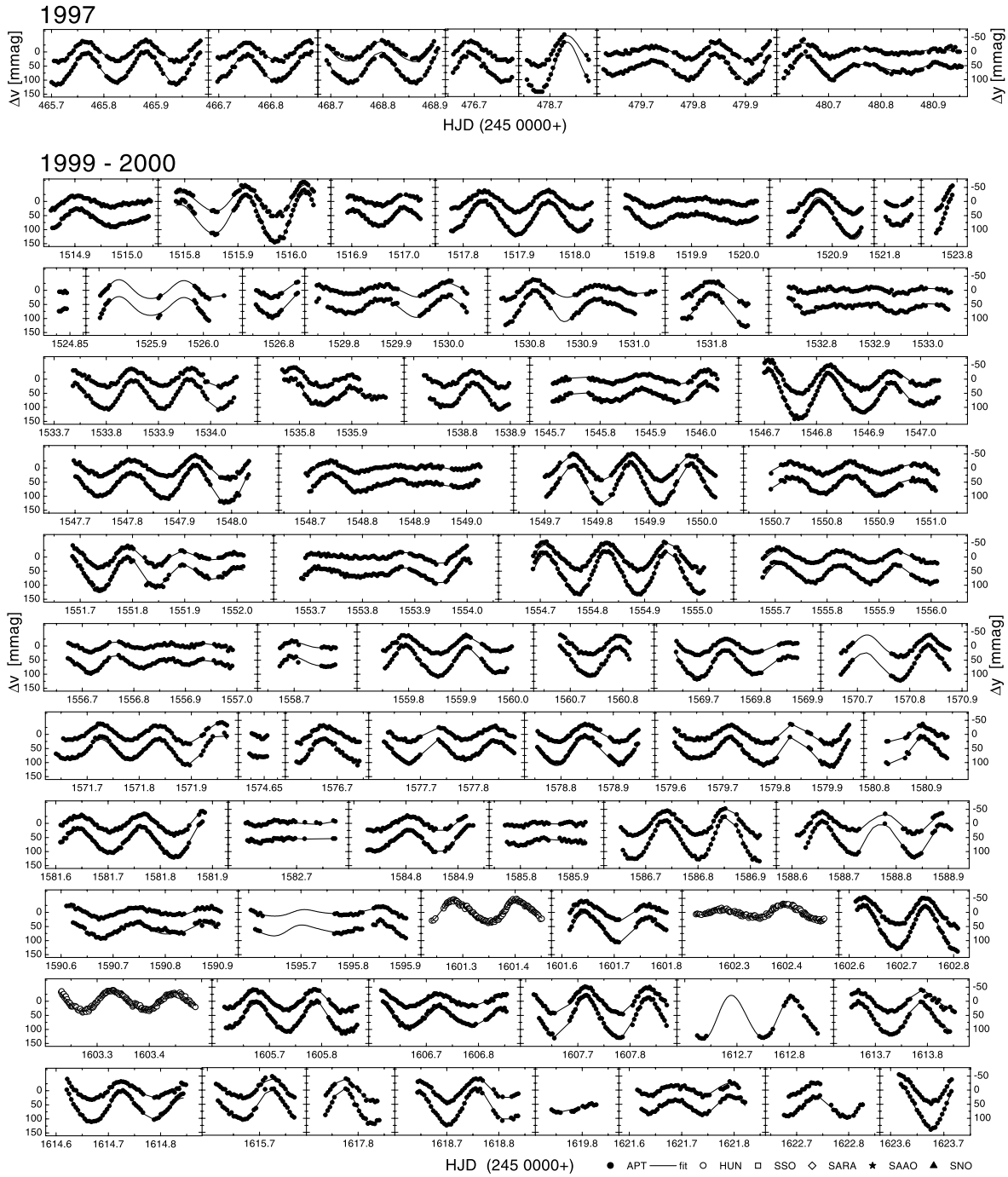

Figure 1. Multisite photometry of BI CMi obtained during the 1997 and 1999–2000 DSN campaigns. Δy and Δv are the observed magnitude differences (variable – comparison stars) normalized to zero in the narrowband *uvby* system. The fit of the 29-frequency solution derived in this paper is shown as a solid curve. Filled circles: APT; open circles: Piszkéstető; open rectangles: SSO; filled stars: SAAO; open diamonds: SARA; filled triangles: SNO.

measurements were made through the Strömgren v and y filters to provide a relatively large baseline in wavelength. The three-star technique (Breger 1993), in which measurements of the variable star are alternated with those of two comparison stars, was adopted. Since the same photometric channel is used for all three measurements, the procedure can produce the required long-term stability of 2 mmag or better. For the PMT measurements, two comparison stars, HD 66925 and HD 66829, were used. HD 66925 has been used as a comparison star before by Mantegazza & Poretti (1994), who found no variability. HD 66829 was used by them as a second comparison star for only two nights, after a previously used comparison star was found by them to be a microvariable. In a later section we will show that the early F star, HD 66829, also exhibits microvariability of about 2 mmag. The time-scale of this variability is consistent with a γ-Doradus type of variability, known to occur at this spectral type (e.g. see Kaye et al. 1999). Consequently, the star was only used for short-term smoothing of the unavoidable scatter of the measurements of the comparison star, HD 66925.

The following telescopes were used:

(i) The 0.75-cm Vienna Automatic Photoelectric Telescope (APT), situated at Washington Camp in Arizona, USA, was used

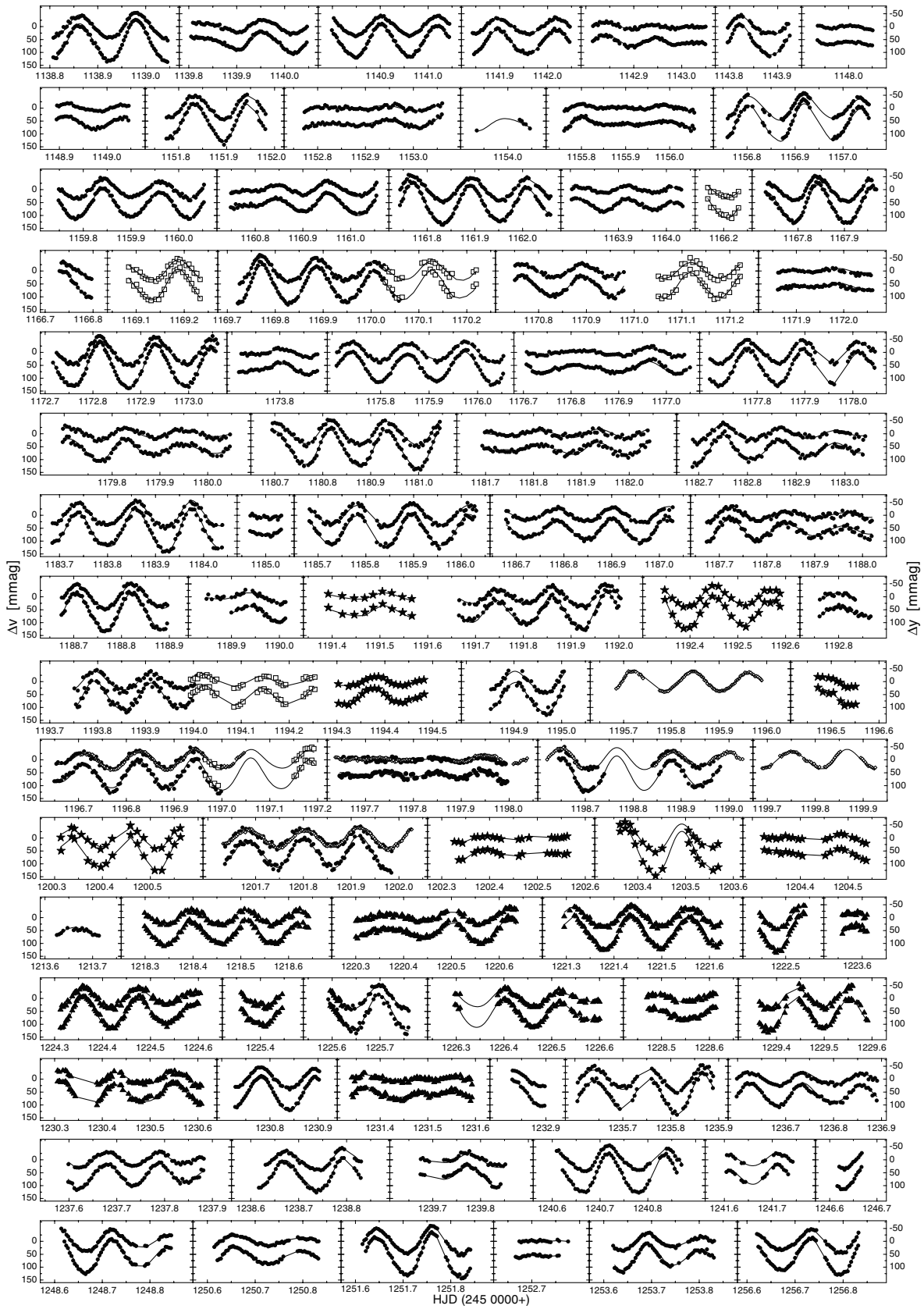

Figure 2. Multisite photometry of BI CMi obtained during the 1998–1999 DSN campaign. See previous figure for details.

(see Breger & Hiesberger 1999). Details on the observations, reductions and results for the present campaign can be found in Rodler & Handler (2001).

(ii) Observations from the Observatorio de Sierra Nevada (OSN), located at 2900 m above sea level in the south-east of Spain, were made using the simultaneous four-channel *uvby* Strömgren photoelectric photometer attached to a 0.9-m telescope. The telescope and photometer are automatically controlled by software developed at the Institito de Astrofisica de Andalucia. A PMT detector was used. The measurements consisted of 30-s integrations using a 30-arcsec diaphragm. Reductions were made using software installed at OSN giving standard magnitude differences.

(iii) Differential single-channel v and y photometric observations were acquired on eight nights in 1999 January using the modular photometer attached to the 0.5-m telescope of the SAAO (South African Astronomical Observatory). The detector used in these observations was a Hamamatsu AE733 GaAs photomultiplier with a system dead time of 30 ns. Photometric diaphrams of 30–40 arcsec were used, depending on the telescope's tracking performance and on the seeing.

(iv) The 60-cm reflector at Siding Spring Observatory was used with a PMT detector and the Johnson V and the Strömgren v filters.

(v) The 0.9-m Southeastern Association for Research in Astronomy (SARA) telescope, located at Kitt Peak National Observatory in Arizona, USA, was equipped with a CCD camera, consisting of an Apogee AP4 and a Kodak KAF–4200 grade 0 2048 × 2048 chip, binned 2 × 2. The image scale was 0.5 arcsec per binned pixel. Read noise was approximately 30 e^- rms, and the gain 6.7 e^- ADU^{-1}. The CCD measurements made by M. Wood, were reduced by K. Bischof in the standard fashion with the APPHOT routines of the IRAF[1] package. This included bias subtraction, flat-field division, sky subtraction, and choosing the optimum aperture size (diameter ∼12 pixels). All the stars brighter than the twelfth magnitude present on the CCD frames were examined: four relatively bright objects were found to be non-variable and were selected as comparison stars.

The SARA CCD measurements had an excellent coverage with a data point every 40 s. This seeming advantage of a large number of measurements is offset by the fact that the observational errors of successive measurements are not independent of each other: the deviations are systematic. Consequently, we feel justified in grouping together a number (∼7) of successive measurements to simulate the coverage from the other observatories. A positive side effect is the reduction in the average residuals of these CCD measurements, so that they could be given full weight in the multifrequency solutions.

(vi) The 1-m telescope at the Piszkéstető Observatory in Hungary was used together with a CCD photometer. The high-accuracy data were reduced in the same way as the SARA measurements (above).

Table 1 provides the journal of observations. The light curves are shown in Figs 1 and 2, which also include a comparison with the fit derived in the next section.

[1] IRAF is distributed by the National Optical Astronomy Observatories, which is operated by the Association of Universities for Research in Astronomy, Inc., under contract to the National Science Foundation.

3 DETECTION OF THE PULSATION FREQUENCIES

The pulsation frequency analyses were performed with a package of computer programs with single-frequency and multiple-frequency techniques (programs PERIOD, Breger 1990; PERIOD98, Sperl 1998), which utilize Fourier as well as multiple least-squares algorithms. The latter technique fits a number of simultaneous sinusoidal variations in the magnitude domain and does not rely on pre-whitening. In a previous paper (Breger et al. 1993) we argued that a ratio of amplitude signal/noise = 4.0 provides a useful criterion for judging the reality of a peak. For the detection of frequency combinations, such as the $2f$ term, the criterion was relaxed to 3.5, since the frequency values during the search are already known (for more details see Breger et al. 1999).

For the frequency detection, we combined the y (9011 new measurements) and v data (8220 new measurements). The dependence of the pulsation amplitude on wavelength was compensated by multiplying the v data set by an experimentally determined factor of 0.632 and increasing the weight of the data points by 1/0.632. This scaling creates similar amplitudes but does not falsify the power spectra. Note that different colours and data sets were only combined to detect new frequency peaks in the Fourier power spectrum and to determine the significance of the detection. The effects of imperfect amplitude scaling and small phase shifts between colours can be shown to be very small.

A difficulty with detecting and fitting low-amplitude modes concerns the relatively small number of very divergent data points. An example would be a data point with a deviation of, say, 15 mmag. This residual cannot be caused by undetected modes if these have amplitudes of 1 mmag. For the first time, we have included a weighting scheme to de-emphasize the effect of very divergent points. In this very conservative scheme, a full weight of 1.0 is assigned to the vast majority of data points, while the very deviant points are assigned a lower weight. This is done without knowing or being able to justify why a particular point was of poor quality. The following weighting scheme is used when $\sigma(i)$ is the deviation of the ith point from the solution.

For $\sigma(i) \leq$ Limit : Weight$(i) = 1$.

For $\sigma(i) >$ Limit : Weight$(i) =$ (Limit/$\sigma(i)$)**2.

If the weighting limit is chosen correctly and conservatively, such a scheme does not suppress the discovery of additional frequencies. It is important to note that a limit of the same order as the amplitudes to be detected should not be used, e.g. adopting such a weighting scheme is not advantageous for the dominant modes of the star. Furthermore, if the distribution of residuals is Gaussian, then such a weighting scheme is not suitable. For the present data set of BI CMi, there are a number of divergent points beyond the statistically expected number. Consequently, for f_{20} and beyond, the weighting scheme improves the detection efficiency. Experimentation with different limits led us to an admittedly nearly arbitrary limit allowing 80 per cent of the points to have full weight. For our final solutions we have adopted the limits of 7.3 mmag in v and 6.2 mmag in y. This resulted in 81 per cent of the data points having full weight and 7 per cent having a weight of less than 0.5. The deviant points are not completely distributed at random.

To detect the frequencies of pulsation, we have performed Fourier analyses of the combined data. A number of statistically significant peaks were selected in order to compute a

Table 2. The frequency spectrum of BI CMi from 1997 to 2000.

Frequency		Detection Significance	Amplitude v filter			Amplitude y filter		
			1999–2000	1998–1999	1997	1999–2000	1998–1999	1997
cycle d^{-1}	μHz/ID	Ampl. signal/noise	mmag	mmag	mmag	mmag	mmag	mmag
			±0.1	±0.1	±0.3	±0.1	±0.1	±0.3
f_1, 8.2455	95.43	192	36.5	35.7	34.6	22.6	22.5	22.0
f_2, 8.8663	102.62	169	31.5	31.4	31.6	20.0	19.8	20.6
f_3, 8.5134	98.53	53.3	10.0	9.4	10.4	6.5	5.9	6.6
f_4, 7.4244	85.93	46.2	8.9	8.0	6.7	5.4	5.0	4.3
f_5, 10.4289	120.71	33.4	5.8	5.1	5.3	3.8	3.7	2.9
f_6, 10.4365	120.79	21.6	4.3	4.3	4.8	2.4	2.8	2.9
f_7, 7.8839	91.25	15.2	3.0	2.9		1.5	1.9	
f_8, 17.1119	f_1+f_2	18.4	2.6	2.9		1.6	1.9	
f_9, 9.5244	110.23	16.2	2.9	2.8		2.1	1.9	
f_{10}, 4.7826	55.35	11.5	2.4	1.7		1.3	1.3	
f_{11}, 1.6619	19.23	7.5	1.8	1.6		1.4	0.7	
f_{12}, 13.0227	150.73	11.4	1.7	2.2		1.2	1.5	
f_{13}, 8.6577	100.21	12.4	1.5	2.3		1.5	1.6	
f_{14}, 11.2608[a]	130.33	15.0	2.7	1.5	4.4	1.6	0.7	3.3
f_{15}, 17.0266	$=2f_3$	14.2	2.1	1.5		1.4	1.2	
f_{16}, 8.6405	100.01	11.4	1.6	1.7		1.1	1.6	
f_{17}, 4.8178	55.76	8.4	1.6	1.7		0.9	0.9	
f_{18}, 16.4911	$=2f_1$	13.1	1.7	1.7		1.1	1.0	
f_{19}, 10.2413	118.53	8.5	1.7	1.8		0.9	1.3	
f_{20}, 15.6699	f_1+f_4	8.2	1.0	1.3		0.8	0.7	
f_{21}, 12.3500	142.94	8.4	1.2	0.9		0.7	0.8	
f_{22}, 17.7327	$=2f_2$	9.0	0.7	0.9		0.8	0.8	
f_{23}, 6.1776	71.50	5.7	1.2	0.7		0.6	0.6	
f_{24}, 12.8321	148.52	4.4	0.8	1.2		0.5	0.6	
f_{25}, 16.7588	f_1+f_3	5.2	0.8	0.6		0.4	0.6	
f_{26}, 16.2907	f_2+f_4	4.3	0.8	0.7		0.4	0.6	
f_{27}, 9.0988	105.31	5.1	0.6	0.8		0.7	0.7	
f_{28}, 12.3268	142.67	4.1	1.1	0.8		0.4	0.5	
f_{29}, 17.3796	f_2+f_3	3.8	0.5	0.7		0.3	0.5	
Residuals, single measurement			4.5	5.0	4.6	3.8	4.3	4.2

[a] f_{14} has a time-variable amplitude, see text.

multifrequency solution to the observed light curve. For computing multifrequency solutions, the amplitudes and phases were computed separately for each colour, so that even these small errors associated with combining different colours are avoided. Because of the daytime and observing-season (annual) gaps, different alias possibilities were tried out and the fit with the lowest residuals selected.

The resulting optimum multifrequency solution was then pre-whitened and Fourier analyses computed from the residuals. This led a number of new peaks, which were tested for statistical significance. The previous procedure was then repeated. Note that the new multifrequency solutions always were computed from the observed (not the pre-whitened) data.

The analysis was repeated while adding more and more frequencies, until the new peaks were no longer statistically significant. We have also repeated the complete frequency-finding analysis for each observing season and each colour separately, in order to confirm that the detected frequencies are indeed present in all the data. This also made it possible to check for amplitude variability: only one frequency, namely, f_{14}, showed strong amplitude variability. This was taken into consideration for the multifrequency solutions.

29 statistically significant peaks are found with the following properties.

(i) 20 peaks are independent pulsation frequencies in a limited frequency range, which defines a frequency region of pulsational excitation. The region is found to range from 4.8 to 13.0 cycle d^{-1} (55 to 150 μHz).

(ii) A very low frequency of 1.66 cycle d^{-1} is found, which is not a combination frequency.

(iii) Three peaks can be identified with the $2f$ terms of the three dominant pulsation modes.

(iv) Five further frequencies are linear combinations of other frequencies with large amplitudes with a mathematical form, $f_i + f_j$. Our inability to find the corresponding f_i–f_j values is, in large part, connected with the larger observational uncertainties (zero points) in the frequency range below 0.5 cycle d^{-1}.

(v) The value of f_{12} (see Table 2) is related to two other modes by the relation $f_{12} = f_{10} + f_1 - 0.005438$ cycle d^{-1}. The constant is approximately equal to twice the reciprocal of the number of days in a year. It corresponds to approximately twice the separation caused by annual aliasing. We have tested the combination frequency, $f_{10} + f_1 = 13.0281$, and find a much poorer fit of only 1-mmag amplitude (instead of 2 mmag) in v. We can, at this stage, neither confirm nor reject the possibility that f_{12} might be a combination frequency.

Fig. 3 and Table 2 show the results of the multiperiod analysis. In the figure, the various power spectra are presented as a series of panels, each with additional frequencies removed relative to the panel above.

4 IS THE DETECTED LOW FREQUENCY REALLY PRESENT IN BI CMI?

In the previous section, we have detected a low frequency peak at 1.662 cycle d^{-1}. The reliable detection of such low frequencies is

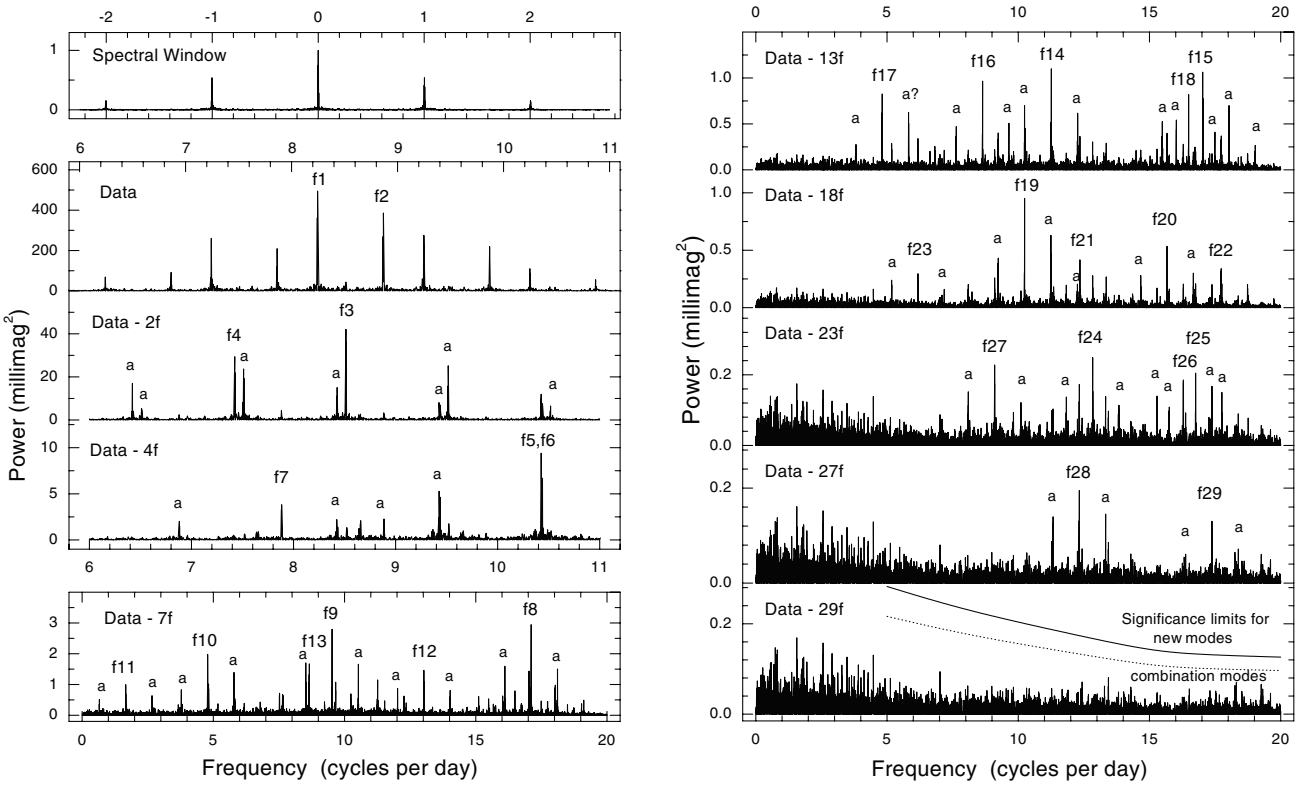

Figure 3. Power spectrum of BI CMi. The spectra are based on the combined 1997–2000 data in both the *y* and *v* colours and are shown before and after applying multifrequency solutions. Some 1 cycle d^{-1} aliases are marked with 'a' for clarity. See text for the numbering scheme and a discussion of significance levels.

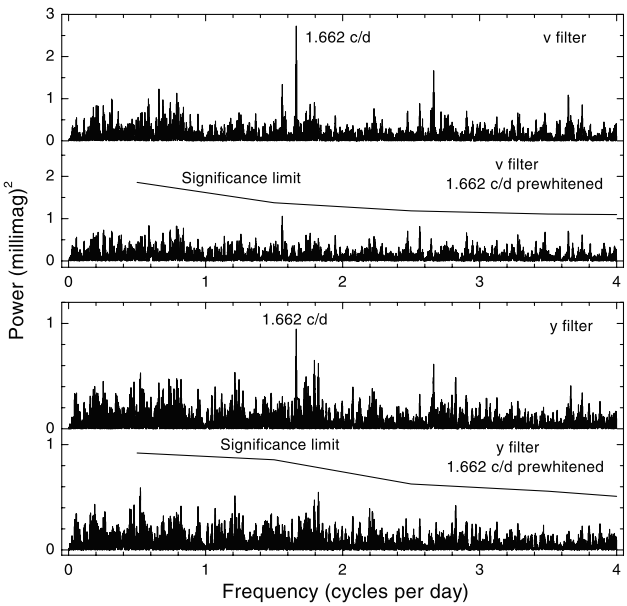

Figure 4. Power spectrum of BI CMi in the low-frequency domain using only data with secure zero-point stability. Results are shown for the two filters, *v* and *y*, separately before and after pre-whitening the 1.662 cycle d^{-1} peak. This shows that the 1.662 cycle d^{-1} peak is present in both filters. Furthermore, only this peak is statistically significant.

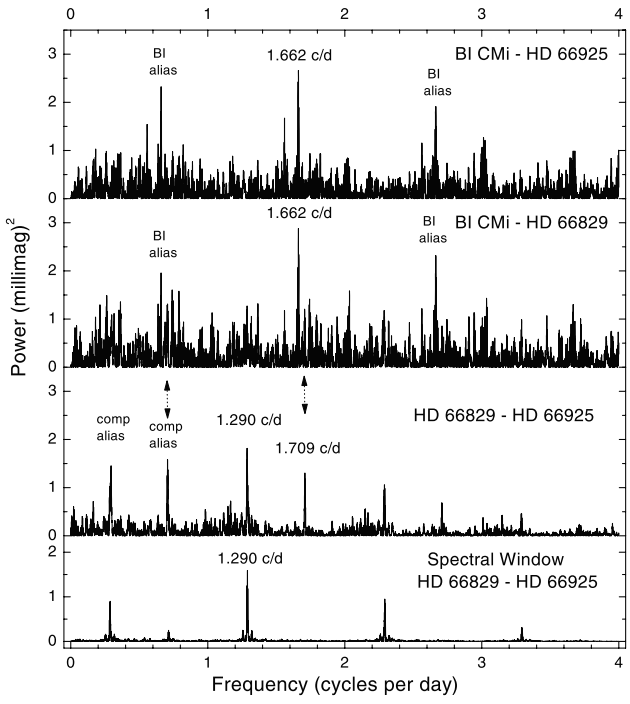

Figure 5. A comparison of the power spectra of the measured magnitude differences in the *v* filter between BI CMi and the two comparison stars used. The origin of a peak can be inferred if it occurs in two (and only two) of these panels. The diagram shows that the 1.662 cycle d^{-1} peak originates in BI CMi, while the 1.29/1.71 cycle d^{-1} combination comes from the early F star, HD 66829.

relatively difficult owing to the higher observational errors in the low frequency domain. In particular, extinction errors, slow zero-point drifts and slowly varying comparison stars can cause spurious frequency detections. In order to examine the reality of this detection, we have re-analysed the 1998–1999 and 1999–2000 data by using only the parts with the most reliable instrument stability, i.e. the available data with zero-point stability of 1 mmag or better. This excludes the block of 29 nights of 1998–1999 APT measurements from JD 245 1169 to 245 1226, the JD 245 1147 night and the three nights of Hungarian CCD data from the 1999–2000 season. For the analysis we have pre-whitened all the known frequencies in the higher-frequency domain in order to avoid spectral leakage.

Fig. 4 shows the Fourier spectrum in the low-frequency domain for the two filters. The 1.662 cycle d^{-1} peak can be seen to be dominant in both filters. We also find that the next highest peaks in BI CMi are not found in both filters and also lie below the formal level of significance.

The possibility that the 1.662 cycle d^{-1} peak originates in one of the two comparison stars still needs to be tested. We have repeated the complete data reduction for the v and y filters. Both filters give similar conclusions, but we will concentrate here on the v filter, which has a higher signal/noise ratio. The photometric differences, (BI CMi – HD 66925), (BI CMi – HD 66829), as well as (HD 66829 – HD 66925) were calculated. The power spectra are shown in Fig. 5. This figure shows the following.

(i) The 1.662 cycle d^{-1} peak is present in both power spectra involving BI CMi, but absent in the difference between the two comparison stars. This confirms that the 1.662 cycle d^{-1} originates in BI CMi.

(ii) HD 66829 shows some microvariability with peaks at 1.290 and 1.709 cycle d^{-1} and its 1 cycle d^{-1} aliases. These peaks are only present in the power spectra involving HD 66829. The time-scales are consistent with a γ Doradus type of variability common in early F stars. Note that, owing to the excellent frequency resolution of the campaign, the peaks at 1.662 (BI CMi) and 1.709 cycle d^{-1} (HD 66829) are clearly separated. We also note that the 1 cycle d^{-1} aliases of these two frequencies are themselves related through an alias, namely, $0.29 + 0.71 = 1.00$. Nevertheless, a spectral window centred on 1.290 cycle d^{-1} cannot explain all the peaks of HD 66829. Consequently, we are not able to pinpoint the exact frequency(ies) of HD 66829. However, a best solution is obtained with a combination of 0.706 *and* 1.287 cycle d^{-1}.

(iii) The difference between HD 66925 and HD 66829 shows considerably lower noise at low frequencies than the differences between BI CMi and each of these stars. Since BI CMi and HD 66829 have similar apparent magnitudes of $V = 9.2$, brightness differences are not the cause. We strongly suspect that the higher noise level of BI CMi is caused by the presence of undetected low-frequency modes in BI CMi. We note here that various frequency combinations, $f_i + f_j$, were detected but that the existence of their expected counterparts, f_i–f_j, could not be shown. We have examined the data for the expected modes: only the peak at f_1–f_4 = 0.821 cycle d^{-1} is seen, while the others are hidden in the noise. This peak is not statistically significant owing to the high noise (i.e. the presence of other peaks). It appears prudent to stop at this point in order to avoid potential overinterpretation of the data.

4.1 Physical cause of the 1.662 cycle d^{-1} variation

We have already noted that the 1.662 cycle d^{-1} frequency of BI CMi could be the result of γ Doradus type variation. This would make the star one of the most evolved γ Doradus candidates known to date (see Handler 1999). However, our data are insufficient for BI CMi being considered a good candidate adopting the criteria of Kaye et al. (1999): there is only one period in the γ Doradus range and no time-resolved spectroscopy is available. Consequently, we cannot prove that γ Doradus pulsations are excited in BI CMi; alternative explanations need to be considered.

Those other possibilities include ellipsoidal variations and abundance spots on the stellar surface. Concerning the latter possibility, it is important to note that our spectral classification from Section 8.2 (F2 IIIp SrEuCr:) suggests that the star is chemically peculiar, which makes a spot hypothesis non-negligible. Assuming a stellar radius of 3.7 $R_\odot$ (see Section 8.2) and a rotation frequency of 1.662 cycle d^{-1}, we obtain a rotational velocity of 310 km s^{-1} and an orbital inclination of $i = 14°$. This leaves little horizon behind which possible spots can disappear, but this would also provide a natural explanation of the small amplitude of the signal. We add that the rotational light curves of Ap stars often show a double-wave variation, which would then yield $i = 29°$, again consistent with the observed variation and basic stellar parameters. Abundance spots on the stellar surface thus remain a viable explanation for the 1.662 cycle d^{-1} frequency of BI CMi.

Turning to ellipsoidal variations, we note that the observed long period (both for single- and double-wave light curves) is also consistent with this hypothesis; it actually fits the observed period–temperature relation for ellipsoidal variables (see Morris 1985) well. The low photometric amplitude can easily be explained with high orbital inclination. However, the amplitude ratios between the v and y filters we find for this frequency (1.28 ± 0.12 for the 1999–2000 season and 2.3 ± 0.3 for 1998–1999) are inconsistent with the equal v and y amplitudes an ellipsoidal variation is expected to produce.

We suggest that the 1.662 cycle d^{-1} variation of BI CMi originates from either pulsation or abundance spots, but more data, in particular time-resolved spectroscopy, are required to settle this issue.

5 ANNUAL PULSATION SOLUTIONS

Now that 29 frequencies have been determined, we can derive the amplitudes and examine the data for amplitude variability. For the extensive 1998–1999 and 1999–2000 observing seasons, we have computed separate 29-frequency solutions for each year and each of the two colours. This approach could not be adopted for the 1997 single-filter (y) data, since only seven nights of observation are available. Even with the frequency values known, a 29-frequency solution contains 58+1 (zero-point) degrees of freedom. In order to avoid an overinterpretation of the data, we have only computed the amplitudes and phases for the dominant modes, f_1 to f_6, and the one mode, f_{14}, with variable amplitudes. For all the other modes, the average amplitude and phase computed from the available y data for all years was assumed in the 1997 solution.

An examination of annual amplitude variability requires a knowledge of the uncertainties associated with the derived values. The expected uncertainties in the values of the derived amplitudes, $\sigma(a)$, can be calculated from the average residuals, $\sigma(m)$, of the fit to the data of N measurements with random errors (for a derivation of the formulae see the appendix in Breger et al. 1999):

$$\sigma(a) = \sqrt{\frac{2}{N}}\sigma(m). \quad (1)$$

The uncertainties computed in this manner are shown with the

amplitudes in Table 2. In order to avoid circular arguments, the listed residuals refer to solutions using data in which extremely deviant points were assigned full weight.

For one pulsation mode, f_{14}, strong annual amplitude variability was detected. For the two extensive data sets (1998–1999 and 1999–2000) the significance of amplitude variability exceeds four standard deviations; the even larger amplitude found for 1997 is less significant because of the relatively small data set for 1997.

We also note the presence of several close frequency pairs, e.g. 10.4289 and 10.4365 cycle d^{-1}. The data are of sufficient resolution to detect such a small separation of 0.008 d, namely, 125 d in 1998–1999 and 109 d in 1999–2000. The double structure was detected through our standard procedure involving pre-whitening detected frequencies and then looking for additional peaks. Nevertheless, we checked the reality of the detections with multifrequency solutions involving the pairs: the pairs gave the lowest residuals. Additional tests to examine the reality of the frequency pairs (as opposed to artefacts caused by insufficient resolution, incorrect analyses and amplitude variability) will be applied in a separate paper, in which the problem of close frequencies in δ Scuti stars will be examined in detail.

6 COMPARISON WITH PREVIOUS RESULTS

Mantegazza & Poretti (1994) presented a multifrequency solution of their BI CMi data with 10 frequencies. It is important to note that some of the frequencies with small amplitudes were not regarded by them as reliable.

If one takes into account the lower frequency resolution and possible 1 cycle d^{-1} aliasing of the previous results, the agreement is good. The 0.149 cycle d^{-1} peak is not seen by us and two other frequencies are 1 cycle d^{-1} aliases: the 9.44 cycle d^{-1} peak probably corresponds to our 10.43 cycle d^{-1} doublet and the 0.66 cycle d^{-1} peak becomes 1.66 cycle d^{-1}. Since our multisite campaign is much more extensive than the previous data, the new values are probably applicable.

As was previously the case for our 1997 data, a 29-frequency solution leads to an overinterpretation of the 1991 data (16 nights) with an unstable solution in which modes artificially increase each other's amplitudes to unrealistic values. Consequently, we have adopted the approach used previously for the 1997 data: (i) we determined the 29 best frequency, amplitude and phasing values for the 1991 to 2000 time period (allowing for annual amplitude variations of f_{14}), and (ii) for 1991, we determined the amplitudes and phasing of f_1 through f_6 as well as f_{14}, while assuming the average values for the many other modes with small amplitudes.

For the dominant six frequencies, the amplitudes found for the other years were confirmed within the observational uncertainties. We conclude that the earlier results are in agreement with our new solutions and that the star BI CMi shows very little amplitude variability.

7 THE ROTATIONAL VELOCITY OF BI CMI

In 1999 December, a high-dispersion spectrum of BI CMi was obtained at Kitt Peak National Observatory with the 0.9-m coudé feed telescope and spectrograph. This spectrum covers a wavelength range slightly larger than 300 Å centred on λ6566, and was obtained using grating A, camera 5, and the long collimator. Filter RG610 was used to block both higher and lower orders. Data were recorded on the F3KB CCD (3k × 1k pixels, 15 × 15 μm pixel size, 75 per cent DQE at 6560 Å). The exposure time was 1200 s, resulting in a signal/noise ratio of about 50. Th–Ar exposures used for wavelength calibration were taken immediately before and after the stellar exposure.

The spectrum was reduced at the National Optical Astronomy Observatories offices in Tucson, Arizona in the standard fashion using IRAF and included optimal aperture extraction, bias subtraction and flat-field division. The spectrum was then continuum-normalized by means of a polynomial fit to known continuum points.

The projected rotational velocity $v \sin i$ of BI CMi was estimated with the program ROTATE (Piskunov 1992). To this end, we calculated a model atmosphere with the semi-automatic tool AAP (Gelbmann et al. 1997), with $T_{\rm eff} = 6800$ K, $\log g = 4.0$ and $[M/H] = 0.5$. The particular choice of parameters does not affect the $v \sin i$ value to be determined. We then matched rotationally broadened theoretical spectra with the observed ones by determining individual $v \sin i$ values for each suitable spectral line, i.e. the strongest, unblended metal lines. We obtained an average $v \sin i = 76 \pm 1$ km s^{-1} from 14 such lines and adopted this result as our final projected rotational velocity of BI CMi.

8 THE EVOLUTIONARY STATUS AND MODE IDENTIFICATIONS OF BI CMI

8.1 The photometric approach

Knowledge of the effective temperature and luminosity are important for the matching of the observed frequency spectrum with pulsation models. It is unfortunate that for BI CMi a unique value of luminosity (or surface gravity) cannot be determined at this time.

The standard method of deriving the important parameters for δ Scuti stars relies on the calibrations of the photometric *uvbyβ* system. For BI CMi, Mantegazza & Poretti (1994) have measured the following values: $b - y = 0.226$, $m_1 = 0.203$, $c_1 = 0.707$, $\beta = 2.734$. Using the standard calibrations for absolute magnitude, we find $E(b - y) = 0.013$, $\delta m_1 = -0.028$, and $M_v = 2.4$. Note that the standard uncertainties in M_v are usually in the vicinity of ± 0.3 mag. If the metals were normal, BI CMi could be identified with a main-sequence dwarf.

However, the luminosity of BI CMi is underestimated by these calibrations, possibly extremely so. The metallicity index, δm_1, indicates that the star is not normal and may belong to a class with unusual surface abundances, denoted in different classification schemes as the δ Del or ρ Pup class (for a review see Kurtz 2000). A property of these stars is that the photometric calibrations do not represent the true luminosity. In extreme cases, the error may even be several magnitudes (e.g. see table 8 in Rodriguez & Breger 2000).

It is possible to improve the photometrically determined absolute magnitude and to estimate a rough correction for δm_1 and the relatively slow rotation of BI CMi. This can be done by using the known Hipparcos parallaxes for other δ Scuti stars. Fig. 7 of Rodriguez & Breger (2000) indicates a correction of ∼0.6 mag based on both the rotational velocity and metallicity measured for BI CMi. We must emphasize again that for chemically peculiar stars these values are very uncertain. We now find a corrected estimate of $M_v \sim 1.8$. This value is similar to that obtained by Mantegazza & Poretti (1994), who corrected for the metallicity effect using earlier estimates for such corrections in the literature.

The model-atmosphere calibrations of Moon & Dworetsky (1985) give $T_{\rm eff} = 7100$ K. Since the measured Balmer jump is not

a correct indicator of luminosity and surface gravity, which led to the correction term to the luminosity, $\log g$ needs to be derived from the corrected absolute magnitude. The evolutionary tracks of Pamyatnykh (2000) indicate a mass of 1.8 solar masses for a star with such a temperature and absolute magnitude, which leads to a $\log g$ value of 3.87. These values indicate a radius of 2.6 solar radii and a rotational frequency, $\Omega \geq 0.58\,\mathrm{rev\,d^{-1}}$. This compares to $0.35\,\mathrm{cycle\,d^{-1}}$ for the frequency difference of two identified $\ell = 1$ modes, f_2 and f_3. An explanation for this contradiction is, again, that the luminosity of the star has been underestimated and that the radius of the star is considerably larger. An alternative explanation would require extremely asymmetric rotational splitting.

A further difficulty with the photometrically determined luminosity comes from the relatively low frequencies. If we adopt the values shown above, the pulsational constant, Q, ranges from 0.025 to 0.068 d, with the dominant modes possessing Q values from 0.037 to 0.039 d. Since the radial fundamental mode has $Q = 0.033$ d, in BI CMi even the dominant modes would have to be gravity modes! Inspection of the frequency spectra of well-studied δ Scuti stars shows this to be improbable.

We conclude that the photometric calibrations are not applicable, even with the estimated corrections for metallicity.

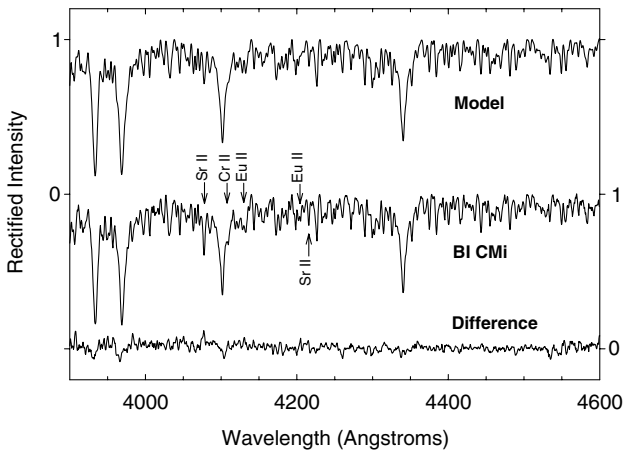

Figure 6. The model fit to BI CMi using the simplex method of Gray et al. (2001), including a difference spectrum between the model and observed spectra. Enhanced lines, owing to Sr II, Eu II and Cr II, are indicated in the spectrum of BI CMi. The scale on the left-hand ordinate indicates the continuum and zero-point levels for the model spectrum, the right-hand scale for the observed spectrum.

8.2 The spectroscopic approach

Spectroscopic analyses confirm that BI CMi is actually an evolved star. In order to investigate the chemical peculiarity and luminosity of BI CMi in more detail, we have obtained a classification–resolution spectrum of BI CMi on the Dark Sky Observatory 0.8-m telescope of Appalachian State University. This spectrum has a spectral range from 3800–4600 Å, a two-pixel resolution of 1.8 Å and signal/noise > 300. We have classified this star on the MK system using standard stars obtained with the same instrumental set-up. The spectrum of BI CMi is a close match to that of β Cas (F2 III), including the K line and the hydrogen lines, except for some chemical peculiarities. The most outstanding peculiarities are an enhanced Sr II λ4077, Eu II (both λ4129 and λ4205 are visibly enhanced), and a possible enhancement of Cr II (there is a line at $\lambda\lambda$4109–4110 which might be Cr II, but this identification is not certain, as it should be closer to λ4111). We give this star a F2 IIIp SrEuCr: classification.

We can obtain an estimate of the basic physical parameters of BI CMi using the multidimensional downhill simplex method developed by Gray, Graham & Hoyt (2001). This method finds the best simultaneous fit to the observed line spectrum and fluxes (from *uvby* photometry) using synthetic spectra and fluxes calculated from Kurucz (1993) models. The resulting fit, illustrated in Fig. 6, gives $T_{\rm eff} = 6925 \pm 75$ K, $\log g = 3.69 \pm 0.10$, $[M/H] = 0.04 \pm 0.10$ and $\xi_{\rm t} = 3.6 \pm 0.5\,\mathrm{km\,s^{-1}}$. These parameters are very similar to those found by Gray et al. (2001) for β Cas ($T_{\rm eff} = 6940$ K, $\log g = 3.65$). We note that the photometric calibrations by Moon & Dworetsky (1985) give similar values for β Cas, namely, $T_{\rm eff} = 6975$ K, $\log g = 3.55$.

If we assign the values of $T_{\rm eff} = 6950$ K, $\log g = 3.6$ to BI CMi, then the Q values of the pulsation modes range from 0.015 to 0.041 d for the non-combination modes, with the dominant mode at 0.022 d, respectively. This corresponds to the value that is expected to the second (± 1) radial overtone and is normal for a δ Scuti star. The temperature and gravity values lead to a radius of 3.7 solar radii for BI CMi together with a rotational frequency, $\Omega \geq 0.40\,\mathrm{rev\,d^{-1}}$. The observed frequency difference ($0.35\,\mathrm{cycle\,d^{-1}}$) of two identified $\ell = 1$ modes, (namely, f_2 and f_3, identified in the next section), is also in agreement.

8.3 Phase difference and amplitude ratios

The campaign was carried out using the v and y filter of the *uvbyβ* system. This allows us to compare the different pulsation modes in the two colours. In particular, the amplitude ratios and phase differences can be used for mode identifications.

Table 3. Phase differences and amplitude ratios for BI CMi.

Frequency cycle d^{-1}	Phase differences in degrees $\phi_v - \phi_y$	Amplitude ratio vy	Probable mode identification
f_1, 8.246	3.48 ± 0.21	1.62 ± 0.01	$\ell = 0$
f_2, 8.866	-0.36 ± 0.24	1.60 ± 0.01	$\ell = 1$
f_3, 8.513	-0.95 ± 0.77	1.58 ± 0.04	$\ell = 1$
f_4, 7.424	-1.13 ± 0.93	1.67 ± 0.05	$\ell = 1$
f_5, 10.429	-6.60 ± 1.36	1.48 ± 0.05	$\ell = 2$
f_6, 10.437	0.91 ± 1.75	1.62 ± 0.08	$\ell = 0$, (1)
f_9, 9.524	-8.04 ± 2.49	1.44 ± 0.09	$\ell = 2$
Uncertain values			
f_7, 7.884	-4.15 ± 2.67	1.72 ± 0.14	$\ell = 2$, 1
f_{10}, 4.783	5.30 ± 4.00	1.59 ± 0.18	$\ell = (0)$

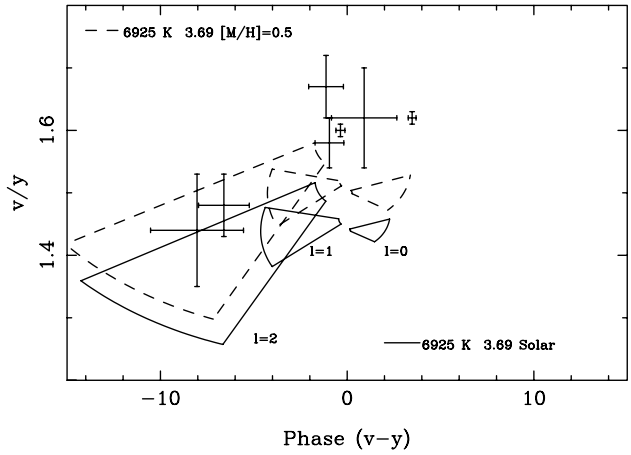

Figure 7. Diagnostic diagram to determine ℓ values from Strömgren v and y colours. Measurements are shown with their error bars, while the loops represent the models for different ℓ values. Note that the phase differences, but not the amplitude ratios, are used for mode identifications.

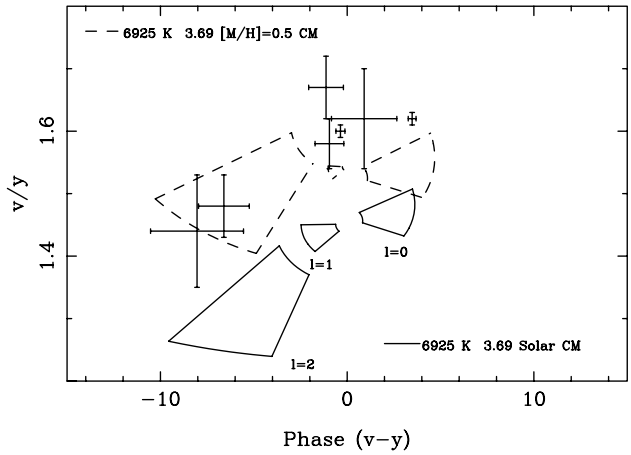

Figure 8. Same as Fig. 7, but with a non-standard treatment of convection from Canuto & Mazzitelli (1992).

Table 3 presents the observed results for the dominant modes of BI CMi. The unavoidable photometric uncertainties do not permit the derivation of reliable values of phase differences and amplitude ratios for the modes with very small amplitudes. The listed uncertainties were calculated from the residuals of the individual data points and assume random errors. To test the validity of the calculated uncertainties, we have subdivided the data into two parts: the 1998–1999 observing season versus the 1999–2000 season with the 1997 data added to this smaller data set. We compared the amplitude ratios and phase differences for both data sets and determined an experimental multiplication factor to the theoretical uncertainties. To our surprise, we obtained a factor of 1.0, i.e. the theoretically computed uncertainties in the amplitude ratios and phase differences are applicable.

Theoretical models to calculate amplitude ratios and phase differences were computed using different assumptions. Fig. 7 shows a comparison of the observed and computed values for two Kurucz stellar atmospheres (6925 K and $\log g = 3.69$, solar composition as well as for enhanced metals of $[M/H] = 0.5$). A phase lag between 90° and 135° and a parameter $R = 1$ to 0.1 have been assumed to calculate the regions where the different ℓ values are more probably located. These values of phase lag and R describe δ Scuti stars very well (Garrido 2000). Note that the higher metal content only increases the amplitude ratios, but does not affect the phase differences in a significant way. The reason is that for models containing more metals, the derivatives with respect to temperature, used for the computation of amplitude ratios, increase differentially more when one goes to shorter wavelengths.

We have also computed models with a non-standard treatment of convection from Canuto & Mazzitelli (1992). This is shown in Fig. 8. The net effect of this change is the increase of the vy ratio, but not the phase differences. The phase depends only on the phase lag, which is usually between 90° and 150° for δ Scuti stars, as well as on the size of the frequency.

The uncertainties based on different assumptions in the models, as well as the luminosity of BI CMi, mostly affect the size of the amplitude ratios, but have little effect on the phase differences. Consequently, the phase differences are the main diagnostic tool to identify the ℓ values. We note a good match with observations for the phase differences, but the computed amplitude ratios are too small.

8.4 Mode identifications

Table 3 lists the results of the mode identifications based on the observed phase differences. The photometrically identified modes range from $\ell = 0$ to 2. This result is typical for δ Scuti stars. The two dominant modes have $\ell = 0$ and 1.

At this stage we would like to defer a detailed discussion of the excited modes to later investigations, for which a variety of specific pulsation models will be computed to compare with the observations.

9 CONCLUSION

The results of this paper can be summarized as follows.

(i) The multisite campaign of BI CMi from 1997 to 2000 was characterized by excellent frequency resolution and high photometric accuracy. 1024 h obtained during 177 nights were used. This campaign utilized both photomultiplier and CCD photometry. The results from the two detectors could be combined at millimagnitude precision.

(ii) The early F star, HD 66829, which had been intended to be used as a second comparison star, was found to be a γ Doradus star with a millimagnitude amplitude.

(iii) For BI CMi, 29 pulsation frequencies could be extracted. These include 20 pulsation modes in the main pulsation frequency range from 4.8 to 13.0 cycle d^{-1} (55 to 150 μHz), eight linear combinations of other frequencies, and a very low frequency at 1.66 cycle d^{-1}.

(iv) The value of the low frequency at 1.66 cycle d^{-1} cannot be identified with a linear combination of other frequencies. Elliposidal variations can be excluded. The most likely explanations are pulsation or abundance spots. If pulsation is the origin, then BI CMi would be both a δ Scuti and a γ Doradus star, which is interesting considering its location in the Hertzsprung–Russell diagram: it is the range where both types of pulsators are found (near the cool edge of the classical instability strip). However, alternative explanations for this long-period variability need to be considered as well.

(v) Another outstanding property of BI CMi is the presence of a

number of close frequency pairs in the power spectrum with separations as small as 0.01 cycle d^{-1}.

(vi) A rotational velocity of $v \sin i = 76 \pm 1\,\mathrm{km\,s^{-1}}$ was determined from a high-dispersion spectrum. We classify the star to have the spectral type of F2 IIIp SrEuCr:.

(vii) From phase differences, the dominant modes can be identified with ℓ values from 0 to 2. Arguments in favour of BI CMi being an evolved δ Scuti star such as 4 CVn and β Cas have been presented.

Further work presently under way involves the examination of the extremely close frequency pairs as well as modelling the detected frequencies with pulsation models.

ACKNOWLEDGMENTS

It is a pleasure to thank Dr Margit Paparó for helping to organize the Hungarian observations and Dr Mike Montgomery for helpful discussions. This investigation has been supported by the Austrian Fonds zur Förderung der wissenschaftlichen Forschung.

REFERENCES

Breger M., 1990, Comm. Asteroseismol., 20, 1
Breger M., 1993, in Butler C. J., Elliott I., eds, Stellar Photometry – Current Techniques and Future Developments. Cambridge Univ. Press, Cambridge, p. 106
Breger M., Beichbuchner F., 1996, A&A, 313, 858
Breger M., Hiesberger F., 1999, A&AS, 135, 547
Breger M., Stich J., Garrido R. et al., 1993, A&A, 271, 482
Breger M., Handler G., Garrido R. et al., 1999, A&A, 349, 225
Canuto V. M., Mazzitelli I., 1992, ApJ, 389, 724
Garrido R., 2000, in Breger M., Montgomery M. H., eds, ASP Conf. Ser. Vol. 210, Delta Scuti and Related Stars. Astron. Soc. Pac., San Francisco, p. 67
Gelbmann M., Kupka F., Weiss W. W., Mathys G., 1997, A&A, 319, 630
Gray R. O., Graham P. W., Hoyt S. R., 2001, AJ, 121, 2159
Handler G., 1999, MNRAS, 309, L19
Kaye A. B., Handler G., Krisciunas K., Poretti E., Zerbi F. M., 1999, PASP, 111, 840
Kurpinska-Winiarska M., Winiarska M., Zola S. T., 1988, IBVS, 3275
Kurtz D. W., 2000, in Breger M., Montgomery M. H., eds, ASP Conf. Ser. Vol. 210, Delta Scuti and Related Stars. Astron. Soc. Pac., San Francisco, p. 287
Kurucz R. L., 1993, CD-ROM 13, ATLAS9 Stellar Atmosphere Programs and 2 $\mathrm{km\,s^{-1}}$ Grid. Smithsonian Astrophys. Obs., Cambridge
Mantegazza L., Poretti E., 1994, A&A, 281, 66
Moon T. T., Dworetsky M. M., 1985, MNRAS, 217, 305
Morris S. L., 1985, ApJ, 295, 143
Pamyatnykh A. A., 2000, in Breger M., Montgomery M. H., eds, ASP Conf. Ser. Vol. 210, Delta Scuti and Related Stars. Astron. Soc. Pac., San Francisco, p. 215
Piskunov N. E., 1992, in Glagolevskij Y. V., Romanyuk I. I., eds, Stellar Magnetism. Nauka, St Petersburg, p. 92
Rodler F., Handler G., 2001, Comm. Asteroseismol., 140, 27
Rodriguez E., Breger M., 2000, A&A, 366, 178
Sperl M., 1998, Comm. Asteroseismol., 111, 1

This paper has been typeset from a TEX/LATEX file prepared by the author.